Presented at the 6th Workshop on RF Superconductivity, CEBAF, Newport News, VA, USA, October 4-8, 1993.

A New Limit to the Maximum RF Magnetic Field for Niobium†

J. Graber‡, N. Black, H. Padamsee, M. Pekeler‡
Laboratory of Nuclear Studies
Cornell University
Ithaca NY 14853

I. INTRODUCTION

What is the maximum RF magnetic field below which niobium will remain superconducting? The highest RF magnetic field at which superconductivity persists for niobium has been reported to be 160 mT for continuous wave (CW)[1] and 165 mT for pulsed operation,[2] both experimental results around 1.5 K. When extrapolated to $T = 0$ K with the usual parabolic dependence, the maximum $B_{RF\text{-}critical}$ ($T = 0$ K) to date was 170 mT. In this work we show that the RF critical magnetic field at $T = 0$ K must be no lower than a range from 231 to 245 mT. This value is also somewhat higher than the theoretical prediction.

II. THE CHALLENGE OF REACHING HIGH MAGNETIC FIELDS

The difficulty with trying to reach high RF magnetic fields in niobium microwave cavities is that one is usually stopped by phenomena such as thermal breakdown, originating at a small imperfection located in the high magnetic field regions of the cavity, or by field emission currents emanating from the high electric field regions. Both mechanisms absorb the available RF power, but thermal breakdown is more severe.

If thermal breakdown is reached at a spot in a high magnetic field, a fast rising pulse of high power makes it possible to continue raising the field, at the expense of an expanding normal conducting (NC) region. With this approach, it becomes possible to impose higher surface fields on other regions of the SC surface that are still superconducting. Hence the usual thermal breakdown field limiting mechanisms can be superseded by pulsed high power. Of course the Q_0 of the cavity at the high field is substantially lower, because of the growing NC region and increasing field emission currents.

Previous analysis[3] of the HPP phenomena has shown that thermal breakdown of the superconducting surface occurs in times which are slow enough that the field level at which thermal breakdown occurs in CW conditions was exceeded by up to 40% for times on the order of tens of microseconds.

Therefore, to reach high fields in spite of field emission and thermal breakdown, we use high power (typically 100 - 150 kilowatts). In order to surpass local thermal breakdown, the filling time of the cavity ($\tau = Q_L/\omega$) is shortened by lowering the loaded quality factor of the cavity (Q_L defined by $1/Q_L = 1/Q_{ext} + 1/Q_0$), which is accomplished by lowering the quality factor (Q_{ext}) of the input coupler. Q_{ext} is decreased by driving the coupling antenna closer to the iris opening of the cavity. Q_{ext} values are adjustable from 10^{10} to 10^6. To withstand the high power levels in the low temperature environment, we use short pulses (100 to 500 μs) at a low rep rate (1 Hz), so that the average power is low (tens of watts).

Experience with high pulsed power operation of SC cavities has shown that high fields can be reached in spite of field emission loading. If the high power is available it is possible to access high fields even though the unloaded quality factor (Q_0) of the cavity falls with the exponentially rising emission currents. More importantly, at the higher field levels, some sources emit so much current that they self destruct, or *process*. Sources of field emission are eliminated by an explosive mechanism. Once the emission current decreases, higher fields can be reached and more sites

destroyed. A complete description of the processing phenomena can be found in the Ph.D. dissertation which covered HPP processing of 3 GHz RF cavities.[2]

III. The Method For Determining E_{PEAK}

The field level reached during pulsed operation depends on the power, the pulse length (t_{RF}), Q_{ext} and Q_0 as follows. At a given incident power level (P_{inc}), the equilibrium (CW) field reached would be:

$$E_{peak}\Big|_{t\to\infty} = \frac{E_{peak}}{E_{acc}}\sqrt{\left(\frac{4\beta}{(1+\beta)^2}\right)\left(\frac{P_{inc}}{L}\right)\left(\frac{R}{Q}\right)Q_0} \tag{1}$$

where E_{peak} is the peak electric field on the surface of the cavity, E_{acc} is the average accelerating gradient experienced by a particle traversing the cavity in phase with the cavity fields (equal to 0.5 * E_{peak} in the cavities tested here), Q_0 is defined above, β is the input coupling factor (equal to Q_0/Q_{ext}), P_{inc} is the power incident on the cavity, L is the active length of the cavity (5 cm for these cavities), and R/Q is the shunt impedance - a geometrical constant useful for defining the accelerating field (2100 Ohms/m in these cavities). This equation is valid for the cavity fields under steady state or CW conditions. A fixed output probe is calibrated for electric field level during CW measurement, in order to measure the fields under transient (pulsed) conditions.

In pulsed operation, the field at time t_{RF} is given by

$$E_{peak}(t_{RF}) = E_{peak}\Big|_{t\to\infty}\left(1-\exp\left[-\frac{t_{RF}}{2\tau}\right]\right) \tag{2}$$

where τ is the cavity's characteristic filling time, as defined above. In the cavities studied here, the peak surface magnetic field is related to the peak electric field by the relationship:

$$\frac{B_{peak}}{E_{peak}} = 2.3\frac{\text{mT}}{\text{MV/m}} \tag{3}$$

IV. The Method For Determining Q_0

During the short RF pulse, the Q_0 cannot easily be determined, although the instantaneous field is known at all times. The extreme coupling of the input antenna to the cavity at the start of the RF pulse is the source of the difficulty. Q_0 measurement is also exacerbated by transient nature of the dissipative phenomenon such as field emission or thermal breakdown. However the peak field $E_{peak}(t)$ reached is well determined from the transmitted power $P_t(t)$ through the previously mentioned calibrated output probe.

In order to more fully investigate the transient Q_0 of the cavities, we developed an analysis which models the increasing field emission loading and the rapid growth of the NC region during the thermal breakdown process, which will be developed below. From this analysis we successfully reconstruct the measured instantaneous field $E_{peak}(t)$ in the cavity. The reconstructed $E_{peak}(t)$ gives us confidence that the Q_0 (t) is properly modeled.

To obtain Q_0 as a function of total losses, we carried out the following analysis. The dissipated power is composed of the following terms:

$$P_{diss} = P_{SC} + P_{FE} + P_{NC} \tag{4}$$

The first term is the superconducting losses, composed of terms due to both the BCS and residual surface resistances. P_{SC} is derived from the CW Q_0 vs. E_{peak} curve at low fields. The second term in equation 4 is the field emission loss, which is modeled as

$$P_{FE} = a\left(E_{peak}\right)^2 \exp\left[-\frac{b}{E_{peak}}\right] \tag{5}$$

where a and b are obtained by fitting the high field CW Q_0 vs. E_{peak} behavior. The final term in equation 4 is the NC or thermal breakdown loss, and it is modeled as

$$P_{NC} = \frac{1}{2} R_{NC}\left(H_{peak}\right)^2 \pi\left(r_{NC}\right)^2 \tag{6}$$

We assume that the cavity has a single breakdown region which activates at a fixed field H_{BD}. When H_{BD} is surpassed, a circular NC region begins to grow on the RF surface. We find the normal conducting radius r_{NC} via the following:

$$r_{NC}(t) = \int_0^t dt\left(v_{NC}\left[H_{peak}(t)\right]\right) \tag{7}$$

While the fields are increasing, the expansion velocity of the NC region v_{NC} is given by

$$v_{NC}\left[H_{peak}(t)\right] = A + B*\left(H_{peak}(t) - H_{BD}\right)^2 \tag{8}$$

Starting values for A and B are obtained from the simulational program **Transient_HEAT**,[4] and then are varied (over a small range) in order to self-consistently reproduce all data from a given experiment. When the fields begin to decrease due to the growth of the NC region, we maintain v_{NC} at the highest value reached until the surface field falls below 1/2 of the H_{BD}. At this point v_{NC} is allowed to decrease exponentially. This relationship was determined empirically to obtain the best fit to $P_t(t)$.

We emphasize that any other combination of loss mechanisms which sum up to the Q_0 (t) used would be equally valid. The point here is that the trial solution Q_0 (t) which we constructed does produce the experimentally measured $P_t(t)$. We constructed Q_0 (t) from plausible loss mechanisms to estimate how strong is the field emission loading and how large the normal conducting region grows during the high power pulse.

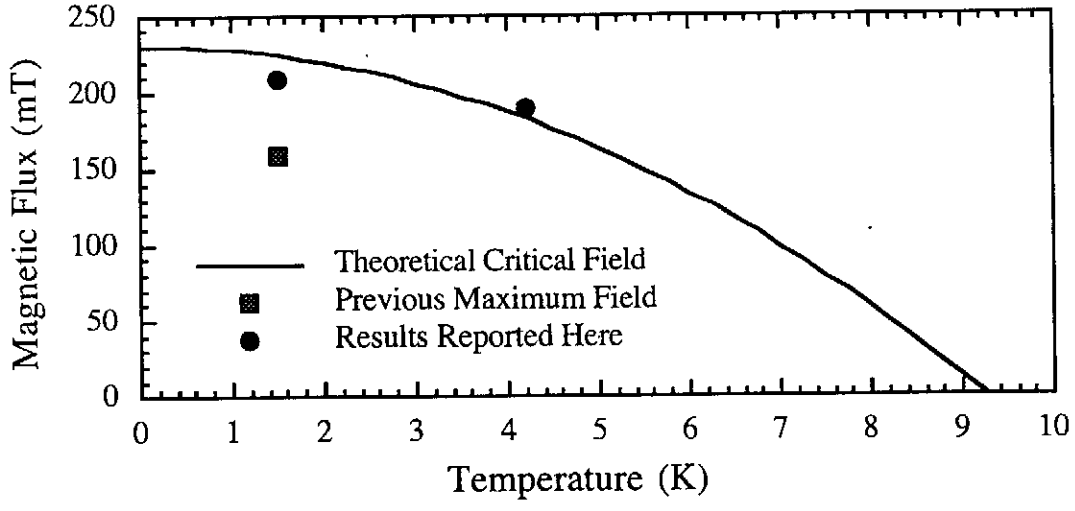

Figure 1. Comparison of the results listed here with the previous maximum measured field, and with the theoretical critical field behavior.

TABLE 1. CW PERFORMANCE OF CAVITIES 1-9 AND 1-10.

Cavity	maximum E_{peak}	Q_0 at max. E_{peak}	Limiting Mechanism
1-9	52 MV/m	8×10^8	Low Q, available power
1-10	58	1×10^9	Field emission, available power

V. RESULTS

In the experiments to be described, we tested two 1-cell 3 GHz cavities. The cavities were made from Russian high RRR Niobium (RRR = 700) in order that the purity, and therefore the thermal conductivity, be as high as possible. By maximizing the thermal conductivity, we delay the onset of thermal breakdown phenomena in the cavities. Table 1 summarizes the CW performance of the two cavities. Table 2 summarizes the pulsed high power performance. Figure 1 shows the theoretically expected parabolic dependence of critical magnetic field with temperature.

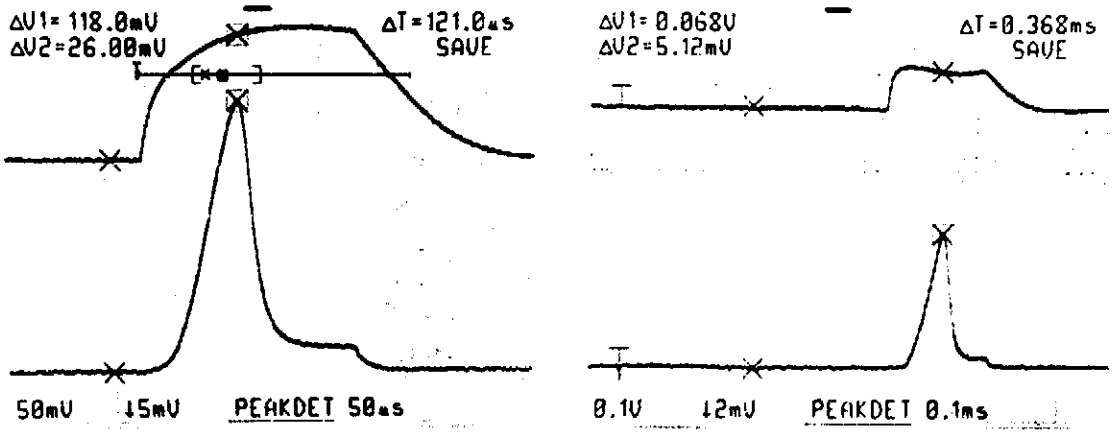

Figure 2. Photographs of oscilloscope traces showing forward and transmitted power during HPP. The left picture is from the experiment with cavity 1-9, with peak P_{inc} = 170 kW, and maximum E_{peak} = 86 MV/m. The right picture is from the experiment with cavity 1-10, with peak P_{inc} = 120 kW, and maximum E_{peak} = 81.5 MV/m.

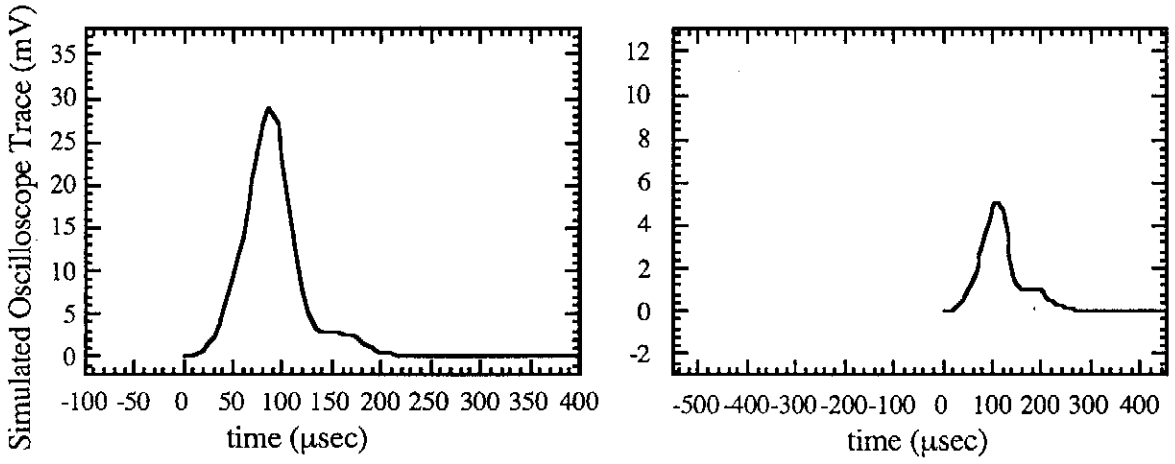

Figure 3. Photographs of oscilloscope traces showing forward and transmitted power during HPP. The left picture is from the experiment with cavity 1-9, with peak P_{inc} = 170 kW, and maximum E_{peak} = 86 MV/m. The right picture is from the experiment with cavity 1-10, with peak P_{inc} = 120 kW, and maximum E_{peak} = 81.5 MV/m.

TABLE 2. PULSED (HPP) PERFORMANCE OF CAVITIES 1-9 AND 1-10.

Cavity	Temp.	P_{RF}	t_{RF}	Q_{ext}	max. E_{peak}	:B_{peak}	t(max E)	Q_0 @ max. E
1-9	1.5 K	150 kW	385 μs	2.8 x 10^6	90.5 MV/m	:208.6 mT	80 μs	8 x 10^6
1-10	1.5	115	300	5.6 x 10^6	82.3	:189.3	110	9 x 10^6
1-10	4.2	130	175	7.0 x 10^6	82.3	:189.3	110	9 x 10^6

The dotted line shows the previous maximum measured magnetic field, and the plotted points are the results of cavities 1-9 and 1-10.

Figure 2 shows two photographs of the experimentally measured transmitted power in the pulsed mode, near the maximum fields obtained. Electric field is proportional to the square root of the transmitted power. The first photo is from the experiment of cavity 1-9, taken at T = 1.5 K, with maximum E_{peak} = 86.0 MV/m. The second photo is from the experiment of cavity 1-10, and was taken at T = 4.2 K, with E_{peak} = 81.5 MV/m.

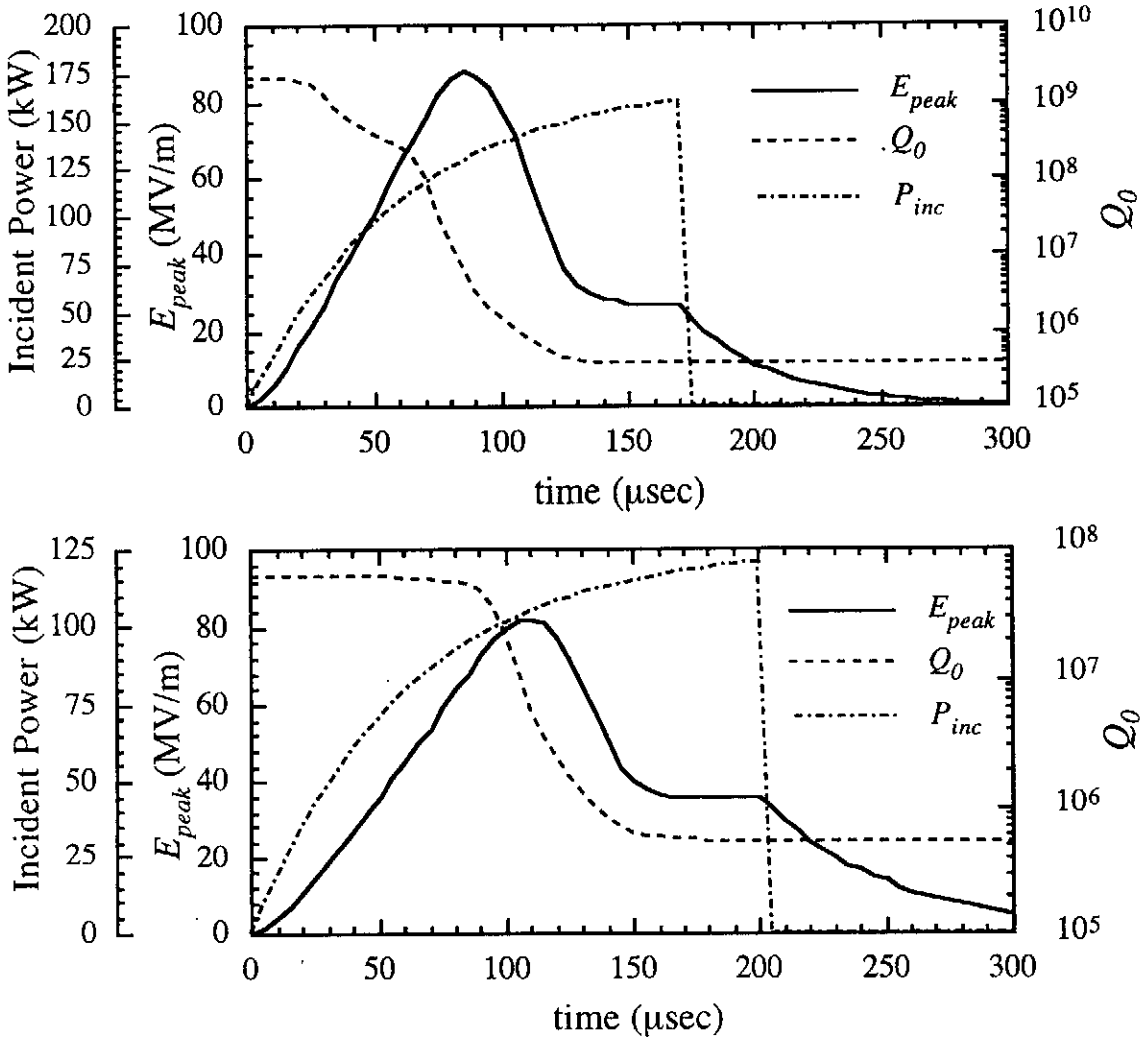

Figure 4. Simulation values of P_{inc}, E_{peak}, and Q_0 shown as functions of time for the two simulations shown in Figure 3. The upper plot here corresponds to the left plot in Figure 3, and the lower plot to the right plot of Figure 3. Inspection shows that at the point of maximum E_{peak}, the Q_0 of the cavity has dropped to only slightly less than 1 x 10^7.

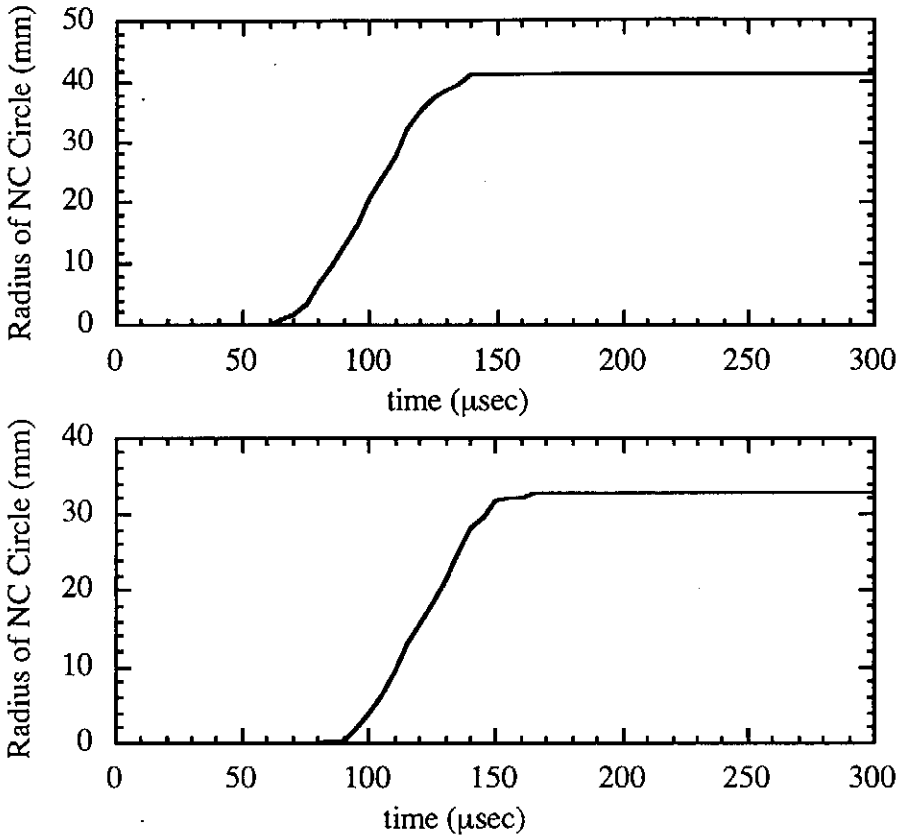

Figure 5. Plots of the simulated radius of normal conducting zone, as a function of time. The plots here correspond to the plots shown in Figures 3 and 4.

We obtained Q_0 at the maximum field in Table 2 by the methods described in the previous section. Figure 3 shows the calculated $P_t(t)$ for each of the photographs shown in Figure 2. Figure 4 shows the applied $P_{inc}(t)$, and the calculated $E_{peak}(t)$ and $Q_0(t)$ for each of the simulations shown in Figure 3.

Figure 5 shows the computed $r_{NC}(t)$ for the simulations shown in the previous two figures. We conclude that at the maximum B_{peak} of Table 2, at least 95% of the cavity area is superconducting. We especially pay attention to the measurements on cavity 1-10 at $T = 4.2$ K. If we use the usual parabolic dependence of $B_{critical}$

$$B_{critical}(T) = \left[B_{critical}(T=0)\right] * \left[1 - \left(\frac{T}{T_{critical}}\right)^2\right] \qquad (9)$$

then with maximum $B(T = 4.2\text{K}) = 189.3$ mT, the zero temperature $B_{RF\text{-}critical}$ for niobium is at least 238.5 mT. We estimate our experimental uncertainty to be approximately 3 MV/m in E_{peak}, corresponding to 7 mT in B_{peak}, therefore we expect the minimum value for $B_{RF\text{-}critical}$ ($T = 0$ K) to be between 231 and 245 mT.

We can further test the validity of our approach by modeling the change in maximum field reached and the time to this maximum. Once the onset of thermal breakdown is crossed, the time to reach the maximum field becomes shorter as the rise time of the fields is increased (in order to exceed the breakdown field). Our model successfully reproduces this behavior. We experimentally measured maximum E_{peak} and $t(E_{peak})$ with Q_{ext} and t_{RF} fixed, and then varied the

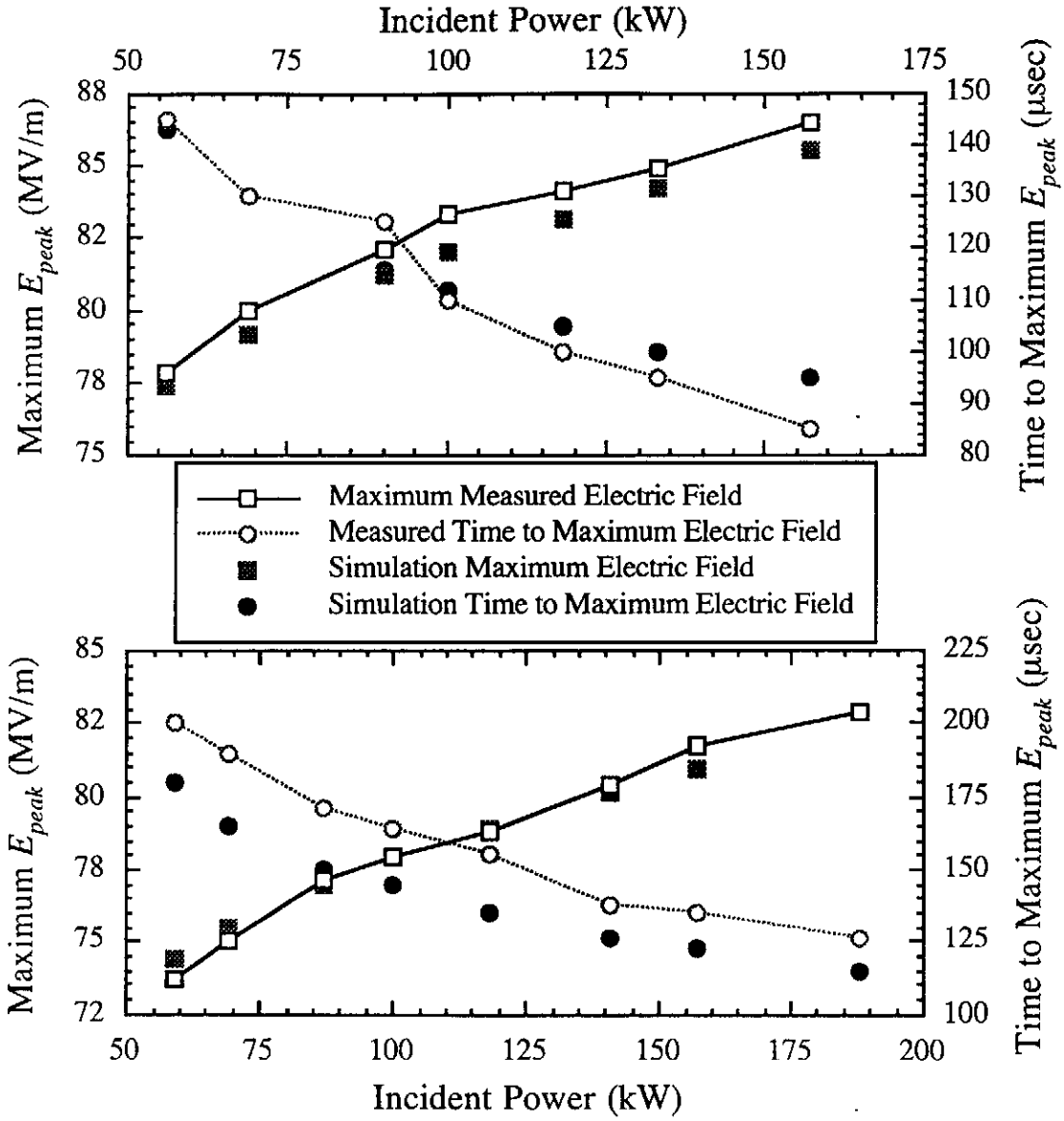

Figure 6. Comparison of measured and simulated maximum E_{peak}, and the time to the maximum value of E_{peak}, as a function of incident power, with all other parameters held constant. The input coupler Q_{ext}'s were 4.7 x 10^6 and 1.0 x 10^7, for the upper and lower plots, respectively. The measurements were made during the experiments on cavity 1-9.

incident power. We ran our simulation under the same conditions. Figure 6 shows two typical examples of the agreement in measured and simulated maximum field and time at which the maximum field is reached. The data for these plots were taken from the experiment on cavity 1-9.

VI. DISCUSSION

Experimentally the RF critical field has been shown to be equal to the superheating critical field (B_{sh}) in Type I superconductors, such as indium, tin and lead. For example, $B_{RF}/B_{critical}$ = 3.5, 3.1 and 1.5 have been measured near T_c for these materials, respectively, in agreement with theoretical predictions for $B_{sh}/B_{critical}$.[5] For Type II alloys such as Sn-In, In-Bi or Nb-Ti, B_{RF} well above H_{c1} has been measured. So it is clear that the field at which DC magnetic flux will first penetrate a Type II superconductor is not the limiting RF critical field. When compared with B_{sh},

the data for the type II superconductors are not as definitive. The error bars are quite large and the measurements were done very near T_c. So the conclusion for type II superconductors that the critical RF field is equal to the superheating critical field is not as strong as for Type I.

The best estimate for Niobium for B_{sh} (0 K) is 210 mT, from experimentally measured values for $B_{critical}$ (0) and κ (T) as discussed in reference 6. Of course this estimate is subject to experimental uncertainties. Our experiments show that B_{RF} critical at 0 K is larger than 231 mT, which is only 11% larger than the superheating field prediction. This is too small a margin to state that the new result is higher than B_{sh}. However the new result is a significant increase over the previous best experimental result B_{RF} (1.5 K) = 170 mT, and perhaps even slightly greater than B_{sh}.

VII. REFERENCES

[1] K. Schnitzke, et. al., *Phys. Lett.*, **45A**, 241 (1973).

[2] J. Graber, Ph. D. Dissertation, Cornell University (1993).

[3] J. Graber, et. al., *Proceedings of the 1993 IEEE Particle Accelerator Conference*, Washington, DC, presented as Poster Paper Sa44, to be published (1993).

[4] X.Cao, *Proceedings of the 5th Workshop on RF Superconductivity*, D. Proch ed., DESY, Hamburg, Germany, **DESY M-92-01**, 727 (1992).

[5] T. Yogi, Ph. D. Thesis, California Institute of Technology (1977), and T. Yogi, et. al., *Phys. Rev. Lett.* **39**, 826 (1977).

[6] G.Müller, *Proceeding of the 3rd Workshop on RF Superconductivity*, K. Shepard ed., Argonne National Laboratory, Argonne, IL, USA, **ANL-PHYS-88-1**, 331 (1988).